KSME

Springer

Journal of Mechanical Science and Technology 34 (11) 2020

Original Article
DOI 10.1007/s12206-020-1032-4

Keywords:
· Critical heat flux
· Inverse heat transfer analysis
· Minimum film boiling
· Quenching
· Surfactant

Correspondence to:
Chi Young Lee
cylee@pknu.ac.kr

Citation:
Kang, D. G., Kim, J. H., Kim, S., Zhang, B. J., Lee, C. Y. (2020). Experimental study on pool boiling regime transitions of vertical rod quenched in aqueous surfactant solutions using inverse heat transfer analysis. Journal of Mechanical Science and Technology 34 (11) (2020) 4753~4761.
http://doi.org/10.1007/s12206-020-1032-4

Received April 17th, 2019
Revised June 28th, 2020
Accepted August 19th, 2020

† Recommended by Editor
Yong Tae Kang

Experimental study on pool boiling regime transitions of vertical rod quenched in aqueous surfactant solutions using inverse heat transfer analysis

Dong Gu Kang[1], Jae Han Kim[2], Sunwoo Kim[3], Bong June Zhang[4] and Chi Young Lee[2,5]

[1]Korea Institute of Nuclear Safety, 62 Gwahak-ro, Yuseong-gu, Daejeon 34142, Korea, [2]Department of Fire Protection Engineering, Pukyong National University, 45 Yongso-ro, Nam-gu, Busan 48513, Korea, [3]Mechanical Engineering Department, University of Alaska Fairbanks, Fairbanks, AK 99775, USA, [4]NBD Nanotechnologies, Inc., 419 Western Avenue, Brighton, MA 02135, USA, [5]Division of Architectural and Fire Protection Engineering, Pukyong National University, 45 Yongso-ro, Nam-gu, Busan 48513, Korea

Abstract In this study, the effect of surfactants and liquid temperature on boiling regime transitions of high-temperature rod during quenching was examined using inverse heat transfer analysis. Liquid pools of the aqueous sodium dodecyl sulfate (SDS) and Triton X-100 solutions were used with pure water. In the present experimental range, the critical heat flux (CHF) and minimum film boiling (MFB) point for all test fluids increased as the liquid temperature decreased. On the other hand, the SDS and Triton X-100 surfactants suppressed the CHF and MFB point, which might be due to the enhancement of vapor film stability caused by reduced surface tension. Some previous experimental studies have reported that the surfactants enhance the boiling regime transitions, but their results seem to be contradictory to the present ones. Considering the present study with the previous works, the surfactants seem to have different effect on boiling phenomena depending on the boiling regime. In other words, in the aqueous surfactant solution, the boiling regime transition points seem to be markedly influenced by a path of boiling regime. In addition, boiling mode diagrams were presented for pure water and aqueous surfactant solutions.

1. Introduction

In order to achieve the higher boiling heat transfer performance, various techniques have been developed and especially applied to a solid surface and a working fluid. For the solid surface, the unique surface treatments such as surface coatings and structured surface fabrication, have been developed and proposed to increase the boiling heat transfer rate [1-6]. It has also been reported that nano-particle deposited surfaces formed by boiling of nano-fluids can increase the critical heat flux (CHF) and boiling heat transfer coefficient [7-15]. These surface treatments change the nucleation site density and surface wettability, and their effect on boiling heat transfer has been extensively studied and confirmed. On the other hand, it is well known that the surface tension of a liquid is one of the important properties affecting the boiling heat transfer. Surfactants have been widely used to change liquid surface tension. Rigorous experimental studies using various aqueous surfactant solutions have been performed to investigate their effect on boiling heat transfer characteristics. However, most of these studies have focused on the nucleate boiling heat transfer regime [16]. There is need for further investigation on other boiling heat transfer characteristics such as CHF and minimum film boiling (MFB) point.

Up to now, a limited number of reports have examined the effect of surface tension on CHF and MFB point by using aqueous surfactant solutions. Borsari and Friedman [17] investigated the effect of surfynol 465 surfactant on CHF and minimum heat flux (MHF) through a voltage-controlled pool boiling experiment using a small platinum wire. Their experimental results

showed that CHF increased and MHF decreased with surfactant concentrations from 0.001 % to 0.405 %. Yang and Maa [18] conducted pool boiling CHF experiments using sodium lauryl benzene sulfonate (SLBS) and sodium lauryl sulfate (SLS). They used the heat flux control method in the experiments. They revealed that an aqueous surfactant solution could increase the CHF value over that of pure water, and that increased surfactant concentration could result in CHF enhancement. Meanwhile, Lin et al. [19] carried out a pool boiling heat transfer experiment using a quenching method. In this experiment, they used the SLS surfactant and copper sphere. Contrary to earlier studies, they reported that the aqueous SLS surfactant solution exhibited the lower CHF and MFB point (i.e., temperature and heat flux) compared to those of pure water. In addition, the CHF and MFB point decreased with increasing concentration of SLS surfactant. Interestingly, both studies of Yang and Maa [18] and Lin et al. [19] used the same SLS surfactant, but their experimental results were contradictory. Considering these findings [17-19], the effect of surfactant on CHF and MFB point seems to be complicated and unclear, and experimental studies on them are still insufficient. Moreover, measures of boiling heat transfer performance such as CHF and MFB point might be sensitive to the types of surfactants. Therefore, additional boiling heat transfer experiments using diverse surfactants should be carried out.

Recently, our research group conducted the quenching experiments using sodium dodecyl sulfate (SDS) and Triton X-100 surfactants [20, 21]. In those works, the quenching curves (time vs. rod center temperature) were obtained from experimental data and the MFB point was solely investigated by using the energy balance equation and lumped system analysis in the film boiling regime. Furthermore, a quantitative comparison between the results using Triton X-100 and SDS surfactants could not be made because their experimental conditions (i.e., initial test specimen temperature and liquid temperature range) were somewhat different.

In the present experimental study, the effect of surfactants and liquid temperature on the boiling heat transfer (e.g., CHF and MFB point) was extensively investigated using the quenching method. In particular, inverse heat transfer analysis [22] was adopted in the study; so the boiling curves (wall temperature vs. heat flux) were constructed from quenching curves (time vs. rod center temperature) for all tests under various liquid temperature conditions. As test fluids, aqueous SDS solutions (1000 wppm and 2000 wppm) and aqueous Triton X-100 solution (100 wppm) were used with pure water. A vertical stainless steel rod was used as a test specimen. The effect of surfactant types on boiling regime transitions was also examined quantitatively. In addition, boiling mode diagrams were presented for pure water and aqueous surfactant solutions.

2. Methodology

2.1 Experiment

The quenching test experimental apparatus in Fig. 1 consists of the test assembly including test specimen and stainless steel tubes, air slide, furnace and its controller, hotplate, beaker, and data acquisition system. Details regarding the experimental set-up, test specimen, and test assembly were described in our previous papers [20, 21]. The temperature of test specimen (50 mm in length and 10 mm in diameter with hemispherical bottom) was measured at its center (25 mm in depth) using a K-type thermocouple (0.5 mm in diameter). Pure water, two aqueous SDS solutions (1000 wppm and 2000 wppm), and aqueous Triton X-100 solution (100 wppm) were used as the test fluids. The properties of the SDS and Triton X-100 surfactants with pure water are summarized in Table 1 [23, 24]. In Table 1, CMC indicates the critical micelle concentration.

Table 1. Properties of SDS and Triton X-100 surfactants with pure water [23, 24].

Property	Pure water	SDS	Triton X-100
Chemical formula	H_2O	$C_{12}H_{25}SO_4Na$	$C_{14}H_{21}(OCH_2CH_2)_{9\text{-}10}OH$
Ionic nature	-	Anionic	Nonionic
Molecular weight	18.0153	288.3	624 (average)
Specific gravity	~1	0.4	1.065
CMC (80 °C)	-	~3000 wppm	~200 wppm
Surface tension (80 °C)	62.673 mN/m	36.5 mN/m (at CMC)	30.9 mN/m (at CMC)
Viscosity (25 °C)	0.89008 cP	-	240 cP

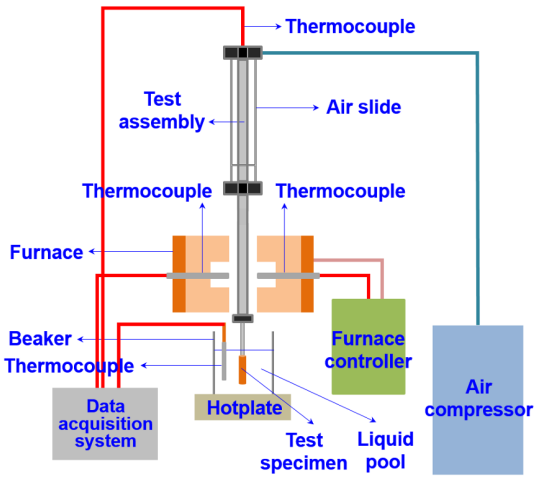

Fig. 1. Quenching experimental set-up [20, 21].

The procedure of experiment was as follows: the test specimen was warmed up to a certain temperature by the furnace, and the liquid pool of 850 ml was also heated to the target temperature by the hot plate. After the furnace and liquid pool reached the steady-state temperature, the test specimen was placed in the high-temperature furnace to heat up to the target temperature of 600 °C. At the moment that the test specimen reached to target temperature, it was dropped into the liquid pool by the air slide. After quenching (i.e., the heat transfer regime of test specimen became to be clearly the single-phase natural convection), temperature data acquisition was stopped

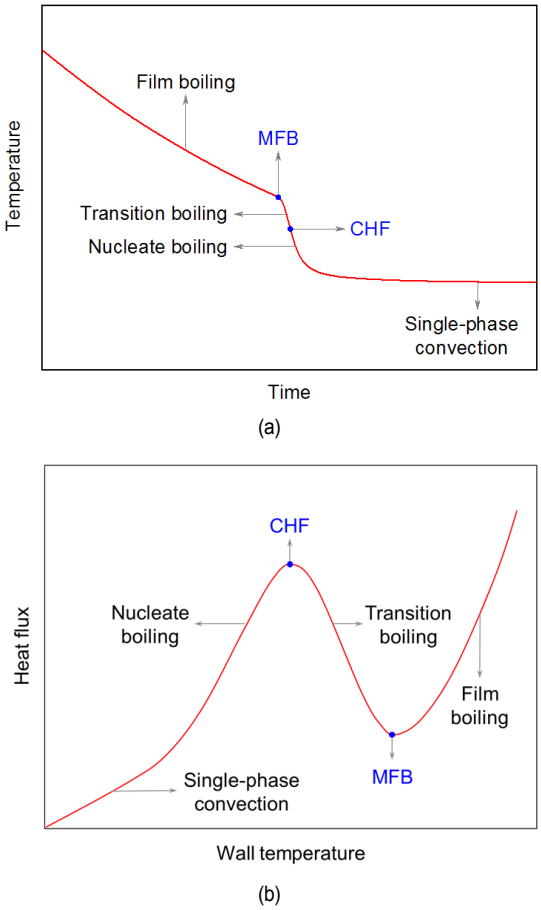

Fig. 2. Schematic of relationship between the typical quenching and boiling curves: (a) quenching curve; (b) boiling curve.

and the experiment was finished. In these experiments, the liquid pool temperature ranged from approximately 56 to 100 °C, and the rod center temperature data with time were stored through the data acquisition system with a sampling frequency of 20 Hz.

In this work, the temperatures of rod center during quenching were measured with time, and quenching curves of time vs. rod center temperature were generated. Based on the quenching curves, the typical boiling curves (i.e., wall temperature and heat flux) could be constructed using the following inverse heat transfer analysis [22].

2.2 Inverse heat transfer analysis

In Fig. 2, the schematic of relationship between the typical quenching and boiling curves is shown. In the quenching curve (i.e., time vs. temperature), the heat transfer regimes are generally altered in turn with time as follows; film boiling, transition boiling, nucleate boiling, and single-phase convection regimes. In Fig. 2(a), those heat transfer regimes are displayed together with the regime transition points (i.e., CHF and MFB points). From such a quenching curve, the boiling curve (i.e., wall temperature vs. heat flux) can be obtained using the inverse heat transfer analysis introduced as below, and the heat transfer regimes with the CHF and MFB points corresponded to those in the quenching curve are shown in Fig. 2(b).

The inverse heat transfer analysis is described as follows: under the assumption of one-dimensional heat conduction, the transient heat conduction equation of the rod (i.e., cylindrical shape) is as below.

$$\frac{1}{r}\frac{\partial}{\partial r}\left(kr\frac{\partial T}{\partial r}\right)=\rho c_{\mathrm{p}}\frac{\partial T}{\partial t} \tag{1}$$

where k, ρ, c_{p}, and t denote the thermal conductivity, density, specific heat, and time, respectively. In addition, r indicates the radial coordinate and r = 0 means the center of rod. In this work, since the temperature at the center of rod was measured, the following boundary conditions are applied.

$$T\left(r=0,t_{\mathrm{i}}\right)=T_{\mathrm{c,i}} \tag{2}$$

$$\frac{\partial T\left(r=0,t_{\mathrm{i}}\right)}{\partial r}=0 \tag{3}$$

where $T_{\mathrm{c,i}}$ denotes the temperature of rod center at the discrete time of t_{i}. Based on Eqs. (1)-(3), the following solution of heat flux (q'') on the surface can be obtained:

$$q''=k\sum_{n=1}^{\infty}\frac{nR^{2n-1}}{2^{2n-1}\left(n!\right)^{2}\alpha^{n}}\frac{d^{n}T_{\mathrm{c}}}{dt^{n}} \tag{4}$$

where α and R indicate the thermal diffusivity and radius of the rod, respectively. A constant thermal diffusivity is assumed. Then, Eq. (4) shows that the solution is a series of derivatives of measured temperature, $T_{\mathrm{c,i}}$, with respect to time. In the present study, the first five derivatives were taken. Due to the nature of inverse heat transfer problem, the calculated heat flux is sensitive to measurement errors. The errors originated at the measurement location (r = 0) propagate to r = R while solving Eq. (1). A larger time step (Δt) mitigates the error propagation. Thus, each set of the experiment data was divided into five sub-sets so that each has the time step of 0.25 s that is five times longer than the original experimental time step of 0.05 s. After each sub-set data was used to compute Eq. (4), all five sets of the computed heat flux values were combined to plot a single boiling curve. The measurement errors and error propagation for all boiling curves reported in this paper were within an acceptable range. Exceedingly large measurement errors must result in scattering points in heat flux vs. wall temperature plots. All heat flux values generated by the inverse heat transfer method used in the present study had a smooth boiling curve, which implies that the measurement errors were well controlled.

In this study, the experimental data (i.e., quenching curves of time vs. rod center temperature) obtained from our previous work [20] using the pure water and aqueous SDS solutions were utilized, and additional quenching experiments using the

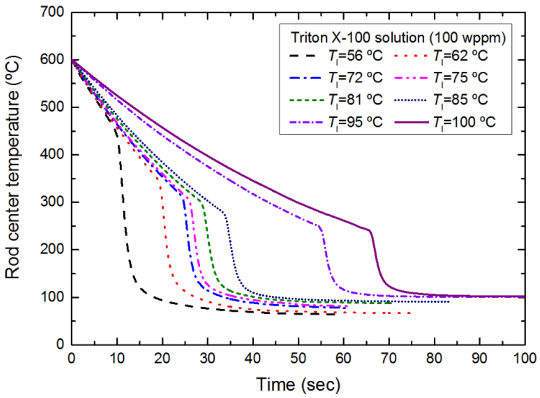

Fig. 3. Typical quenching curve (e.g., aqueous Triton X-100 solution).

aqueous Triton X-100 solution were conducted under similar conditions to our previous work [20]. Using the quenching curves of all fluids under various liquid temperature conditions, boiling curves (wall temperature vs. heat flux) were obtained successfully using the inverse heat transfer analysis.

3. Results and discussion

3.1 Quenching curve

Fig. 3 shows the quenching curves of aqueous Triton X-100 solution at various liquid temperatures. Pure water and aqueous SDS solutions showed similar quenching curves. At the beginning of quenching, the vapor film was formed around the test specimen and film boiling occurred. In this regime, the rod center temperature gradually decreased with time. However, at a certain point in the quenching process called the MFB point, the temperature decreased rapidly and the boiling regime changed from film boiling to transition and nucleate boiling. In this regime, the liquid made contact with the heated surface, resulting in significant increase in the heat transfer rate. The vapor film was replaced with the formation and detachment of numerous vapor bubbles. A few seconds later, the rod center temperature did not decrease substantially and reached almost constant value, indicating the test specimen was sufficiently cooled down and the heat transfer regime had transitioned to single-phase natural convection. As shown in Fig. 3, as the liquid temperature decreased, the quenching duration was shortened and the quenching curve shifted from the right to the left. It means that the temperature gradient in the film boiling regime steepened and the timing and temperature of the MFB point became earlier and increased with decreasing liquid temperature, respectively.

The trend of quenching curve with decreasing the liquid temperature (i.e., decreased quenching duration, steeper temperature gradient in the film boiling regime, and earlier timing and increased temperature of MFB point) resulted from the enhancement of vapor film condensation [20, 21, 25]. As the liquid temperature decreases, condensation in the vapor film can be encouraged, leading to a much thinner vapor film [25], which assists the vapor film to collapse. The heat transfer coefficient in the film boiling regime can be expressed as a function of vapor film thickness, as shown in Eq. (5), under the assumption that heat transfer mainly occurs by conduction across the vapor film in the film boiling regime [26].

$$h = \frac{k_v}{\delta} \tag{5}$$

where h, k_v, and δ are the heat transfer coefficient, thermal conductivity of vapor, and the vapor film thickness, respectively. Therefore, the decrease in vapor film thickness contributes to an increase in heat transfer coefficient by Eq. (5), which leads to a steeper temperature gradient in the film boiling regime.

3.2 Boiling curve

Boiling curves for all test fluids were obtained from quenching curves by using the inverse heat transfer analysis [22] as shown in Fig. 4. The liquid temperature had much influence on the boiling curve. In general, for all test fluids, the heat transfer performance of transition boiling was enhanced by decreasing the liquid temperature. In addition, the CHF and MFB point (i.e., heat flux and temperature) seemed to increase with decreasing liquid temperature.

For some boiling curves, dual humps were observed between film boiling and nucleate boiling regimes, and similar results were reported in previous studies [19, 27]; in Lin et al. [19], dual humps were mainly observed only for water with subcooling ranging from 5 to 30 °C. However, in the present study, the dual humps occurred for the surfactant solutions as well as water. The subcooling range in which they were observed was approximately 8 to 21 °C, which is similar to Lin et al. [19]. Sher et al. [27] investigated the dual peak phenomena with high speed camera. They found that there was a film collapsing noise involving high heat flux and the steam explosion was followed by a “golf-ball” type boiling period. During the “golf-ball” like boiling period, the surface of test specimen was covered by a large number of concaved cells and the heat flux was decreased. Then, as the vapor film was partially collapsed, the boiling regime was transferred to transition boiling.

3.3 Effect of surfactants and liquid temperature on CHF and MFB point

In Fig. 5, the boiling curves for pure water and aqueous surfactant solutions under saturated condition are compared. In the film boiling regime, boiling curves for all test liquids were well-overlapped, which implies that the effect of surfactants on the film boiling heat transfer performance is not significant. The effect of surfactants started to be manifested from the MFB point. The MFB point for pure water formed at a higher temperature and higher heat flux than surfactant solutions. In the transition boiling regime, pure water exhibited a higher heat flux than the aqueous surfactant solutions at a given wall tempera-

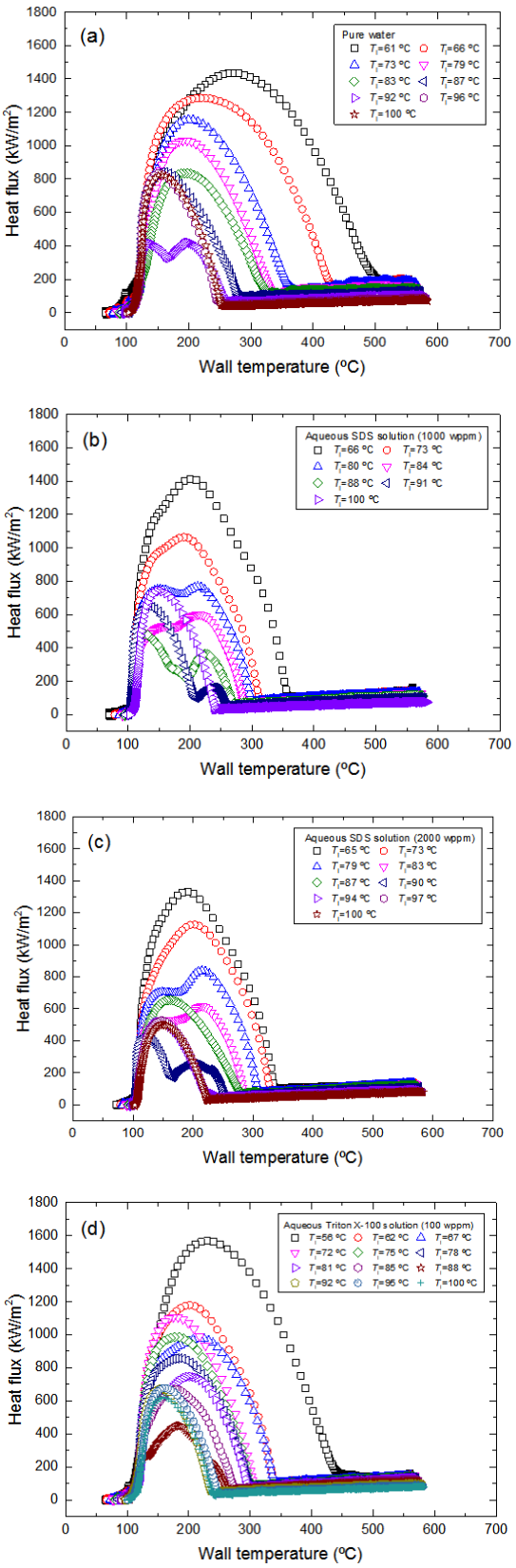

Fig. 4. Boiling curves under various liquid temperature conditions: (a) pure water; (b) aqueous SDS solution (1000 wppm); (c) aqueous SDS solution (2000 wppm); (d) aqueous Triton X-100 solution (100 wppm).

Table 2. Heat transfer performance of SDS and Triton X-100 surfactants with pure water at wall temperature of 200 °C.

Test fluid	Heat flux (kW/m^2)	Heat transfer coefficient (kW/m^2 · °C)
Pure water	646.5	6.47
SDS (1000 wppm)	528.6	5.29
SDS (2000 wppm)	288.0	2.88
Triton X-100 (100 wppm)	454.3	4.54

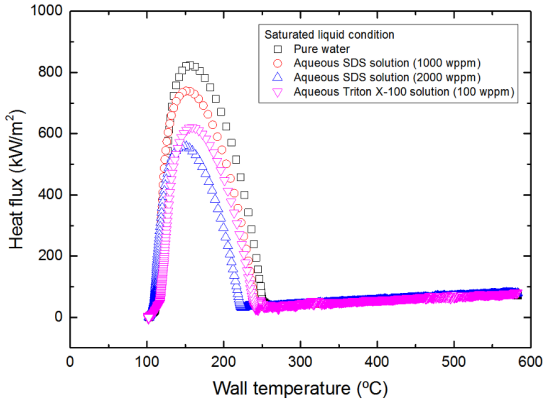

Fig. 5. Comparison of boiling curves for pure water and aqueous surfactant solutions at saturated condition.

ture. As surfactant concentrations increased, the heat flux decreased under saturated condition.

Pure water also had a higher CHF than surfactant solutions. In other words, the SDS and Triton X-100 surfactants reduced the CHF as well as the temperature and heat flux of the MFB point. Table 2 shows the comparison of heat transfer performance with respect to surfactant type and concentration at a given wall temperature of 200 °C (transition boiling regime). Although the concentration of Triton X-100 (100 wppm) was one-tenth or one-twentieth of SDS solutions (1000 or 2000 wppm), the heat transfer performance of the Triton X-100 solution was between those of two SDS solutions in the transition boiling regime. The CHF had the same trend with respect to surfactant concentration and type. This means that the types of surfactants could significantly influence boiling heat transfer performance.

The CHF values of all test fluids at different liquid temperatures are shown in Fig. 6. For clarity, experimental data of boiling curves with dual humps were excluded. As the liquid temperature decreased in the lower liquid temperature range (i.e., below about 90 °C), CHF values of all test liquids increased. However, in the higher liquid temperature range, CHF values did not seem to be changed significantly. Overall, the SDS and Triton X-100 surfactants suppressed the CHF. It is notable that the differences in the CHF values between pure water and surfactant solutions were greater and the effect of surfactant concentration was more apparent at the higher liquid temperature conditions.

Figs. 7 and 8 show the temperature and heat flux of the MFB

point, respectively. General trends of the MFB temperature and heat flux were similar to those of the CHF as shown in Fig. 6 in that they increased with decreasing liquid temperature and pure water showed higher MFB heat flux and temperature than the aqueous surfactant solutions. However, at lower temperature conditions, differences between pure water and surfactant solutions were shown to be greater. There seemed to be no significant differences in the heat flux and temperature of the MFB point among the aqueous surfactant solutions. In addition, Figs. 7 and 8 show the MFB temperature and heat flux compared with those obtained by lumped system analysis in our previous research [20] using Eq. (6).

$$q'' = -\rho c_p \frac{V}{A_s} \frac{\mathrm{d}\Delta T}{\mathrm{d}t} \tag{6}$$

where V, A_s, and ΔT indicate the volume of test specimen, its surface area, and temperature difference between liquid pool and test specimen, respectively. The uncertainties of measurement parameters were estimated using the method of Kline [28], which were within about 2 % for the volume of test specimen, about 2 % for its surface area, about 4 % for temperature gradient with time, and about 9 % for heat flux, respectively. In these figures, the results of SDS 2000 wppm solution are not displayed since those had a similar trend to SDS 1000 wppm solution. As shown in these figures, the MFB temperature and heat flux by lumped system analysis were well-matched to those by inverse heat transfer analysis; the relative differences between the two methods ranged from 0.27 to 3.26 %. However, to obtain extensive information including CHF from the quenching curve and to generate more accurate MFB point information, inverse heat transfer analysis should be utilized.

It is meaningful contribution to discuss the influence of surfactant on boiling regime transitions through the examination of the present and previous [18, 19] experimental results. Based on Figs. 6-8, the SDS and Triton X-100 surfactants resulted in decreasing the CHF and the temperature and heat flux of the MFB point in the present experimental range. As mentioned in the introduction, Yang and Maa [18] and Lin et al. [19] used the SLS surfactant, which is the same as the SDS used in this work [29]. General trends in experimental data from the present study were in agreement with those of Lin et al. [19]. On the other hand, Yang and Maa [18] reported that the SDS surfactant enhanced the CHF value, which contradicts the Lin et al. [19] and present results. Presumably, this discrepancy might be due to differences in experimental details: Yang and Maa [18] used the voltage-controlled (heat flux-controlled) method with nickel wire, while Lin et al. [19] and the present study adopted the quenching method with copper sphere and cylindrical rodlet, respectively. In general, it has been known that surfactants reduce surface tension, which markedly affects the boiling phenomena; the reduction of surface tension prohibits the coalescence of vapor bubbles and improves stability of the liquid-vapor interface.

In the rapid cooling case of the quenching method in Lin et al. [19] and present study, the initial boiling regime is film boiling with vapor film. When the surface temperature gradually decreases in the film boiling regime, the vapor film surrounding the test specimen surface becomes unstable. In other words, major factors influencing the transition process from film boiling to transition boiling might be surface temperature (i.e., vapor generation rate) and vapor film instability (i.e., hydrodynamics such as intermittent liquid contact on surface). Between these two factors, the surfactant has an important effect on vapor-

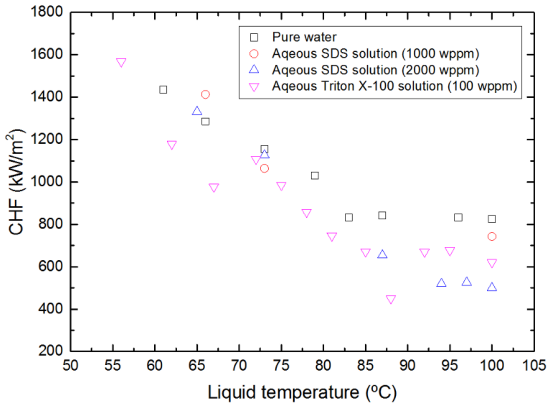

Fig. 6. CHF in pure water and aqueous surfactant solutions.

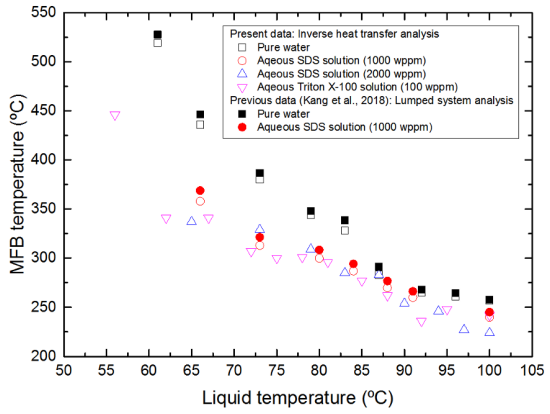

Fig. 7. MFB temperature in pure water and aqueous surfactant solutions.

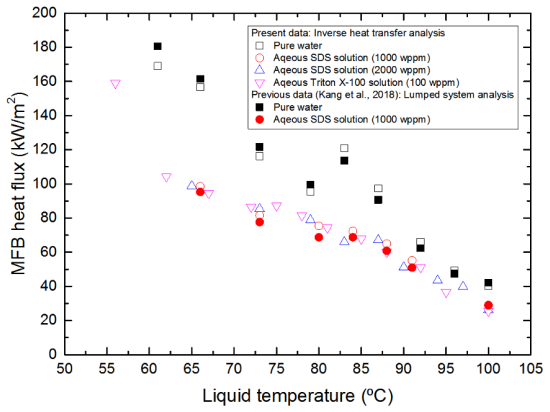

Fig. 8. MFB heat flux in pure water and aqueous surfactant solutions.

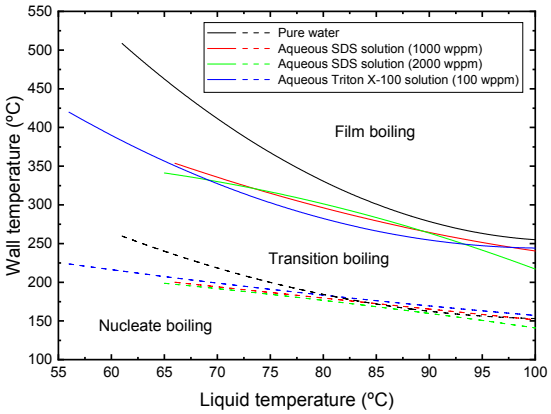

Fig. 9. Boiling mode diagram of pure water and aqueous surfactant solutions.

liquid interfacial hydrodynamics, and it significantly suppresses interfacial oscillatory waves by reducing the surface tension [30]. Therefore, in surfactant solutions, the vapor film can be maintained for a longer time because vapor film stability is enhanced and intermittent liquid contact on the surface cannot occur easily. Therefore, the robustness of vapor film and the delay of vapor film collapse seem to result in reduction of the MFB temperature and heat flux. Even in the transition boiling regime, surfactants might play a role in maintaining the vapor film partially occupying the surface, causing a decrease in CHF.

On the other hand, in the heating case of the heat flux-controlled method in Yang and Maa [18], the initial stage in boiling regimes is a nucleate boiling. As heat flux is increased, vapor bubbles are generated on the surface. A surfactant dissolved in the water has several effect during nucleate boiling. It decreases the surface tension, which contributes to increasing the nucleation rate of vapor bubbles and their departure frequency during boiling. In addition, it inhibits the coalescence of vapor bubbles, so that the formation of vapor film on the surface is prohibited [31]. Hence, the vapor film and hot spot cannot easily form on the surface, which contributes to increasing the CHF.

Considering the present study with the previous works [18, 19, 30, 31], surfactants seem to have different effect on boiling phenomena depending on the boiling regime. In the nucleate boiling regime, surfactants prohibit the formation of vapor film on the surface and enhance boiling heat transfer. But in the film boiling regime, surfactants make vapor film robust and make it difficult for intermittent liquid contact to occur. Hence, in the aqueous surfactant solution, the boiling regime transition points seem to be markedly influenced by the path of boiling regime. For example, the CHF obtained by passing through the nucleate boiling regime (e.g., using the heat flux-controlled method) is higher than pure water, while that through the transition and film boiling regimes (e.g., using the quenching method) is lower than pure water. This behavior looks like hysteresis. However, the effect of surfactants on the boiling regime transitions seems to be still unclear. Therefore, further experiments should be performed using various methods and under various conditions and geometries, which will be conducted as the future work.

On the other hand, boiling mode diagrams for pure water and aqueous SDS and Triton X-100 surfactant solutions relative to wall and liquid temperature are drawn in Fig. 9. They were similar to those proposed by Lin et al. [19]. In this figure, film boiling regime is represented by the regime above the solid line, and nucleate boiling regime is below the dashed line. Transition boiling regime corresponds to the regime between the solid and dashed lines. As shown in this figure, it could be also confirmed that surfactants tend to prolong the film boiling and to delay the entry into nucleate boiling, especially for higher subcooling degrees (i.e., lower liquid temperature ranges). The relative errors between the experimental data and the fitting curve were distributed mostly in the range of -7.6 % to 6.8 %.

4. Conclusions

In order to investigate the effect of surfactants and liquid temperature on CHF and MFB point (temperature and heat flux), quenching experiments using a high-temperature vertical rod were carried out in the liquid pools of pure water, aqueous SDS (1000 wppm and 2000 wppm) and Triton X-100 (100 wppm) solutions. The liquid temperature ranged from approximately 56 °C to 100 °C. Based on quenching curves obtained through the experiments, the heat flux and wall temperature were accurately calculated using inverse heat transfer analysis, and boiling curves were constructed successfully. Concluding remarks are summarized below.

1) From the boiling curves, it was found that heat transfer performance of transition boiling was enhanced by decreasing the liquid temperature, and the CHF and MFB point (temperature and heat flux) for all test fluids increased as the liquid temperature decreased.

2) The aqueous surfactant solutions had lower CHF values than pure water, which was similar to the general trends of MFB temperature and heat flux. One of potential reasons for reduction of the CHF, MFB temperature and heat flux is the delay of vapor film collapse due to enhancement of vapor film stability by the reduced surface tension of aqueous surfactant solutions.

3) Considering the present study with previous works, the surfactants seemed to have different effect on boiling phenomena depending on the boiling regime. In other words, in the nucleate boiling regime, surfactants prohibit the formation of vapor film on the surface and enhance boiling heat transfer. On the other hand, in the film boiling regime, surfactants make vapor film robust and make it difficult for intermittent liquid contact to occur. Therefore, in the aqueous surfactant solution, boiling regime transition points seemed to be markedly influenced by the path of boiling regime.

4) By combining present experimental results, boiling mode diagrams were generated for pure water and aqueous surfactant solutions relative to wall and liquid temperature. It could be

seen from the boiling mode diagrams that surfactants tend to prolong the film boiling and to delay the entry into nucleate boiling, especially for higher subcooling degrees.

References

[1] C. Corty and A. S. Foust, Surface variables in nucleate boiling, *Chemical Engineering Progress Symposium Series*, 51 (1955) 1-12.

[2] C. Li, Z. Wang, P. I. Wang, Y. Peles, N. Koratkar and G. P. Peterson, Nanostructured copper interfaces for enhanced boiling, *Small*, 4 (2008) 1084-1088.

[3] R. Furberg, B. Palm, S. Li, M. Toprak and M. Muhammed, The use of a nano- and microporous surface layer to enhance boiling in a plate heat exchange, *Journal of Heat Transfer-Transactions of the ASME*, 131 (2009) 101010.

[4] D. Saeidi and A. A. Alemrajabi, Experimental investigation of pool boiling heat transfer and critical heat flux of nanostructured surfaces, *International Journal of Heat and Mass Transfer*, 60 (2013) 440-449.

[5] H. T. Phan, N. Caney, M. Philippe, S. Colasson and J. Gavillet, Surface wettability control by nanocoating: the effects on pool boiling heat transfer and nucleation mechanism, *International Journal of Heat and Mass Transfer*, 52 (2009) 5459-5471.

[6] C. Y. Lee, M. M. H. Bhuiya and K. J. Kim, Pool boiling heat transfer with nano-porous surface, *International Journal of Heat and Mass Transfer*, 53 (19-20) (2010) 4274-4279.

[7] H. D. Kim and M. H. Kim, Effect of nanoparticle deposition on capillary wicking that influences the critical heat flux in nanofluids, *Applied Physics Letters*, 91 (2007) 014104.

[8] J. S. Coursey and J. Kim, Nanofluids boiling: the effect of surface wettability, *International Journal of Heat and Mass Transfer*, 29 (2008) 1577-1585.

[9] H. D. Kim and M. H. Kim, Experimental study of the characteristics and mechanism of pool boiling CHF enhancement using nanofluids, *Heat and Mass Transfer*, 45 (2009) 991-998.

[10] H. D. Kim, H. S. Ahn and M. H. Kim, On the mechanism of pool boiling critical heat flux enhancement in nanofluids, *Journal of Heat Transfer*, 132 (2010) 061501.

[11] H. S. Ahn, H. D. Kim, H. Jo, S. Kang and W. Chang, Experimental study of critical heat flux enhancement during forced convective flow boiling of nanofluid on a short heated surface, *International Journal of Multiphase Flow*, 36 (2010) 375-384.

[12] E. Forrest, E. Williamson, J. Buongiorno, L. W. Hu, M. Rubner and R. Cohen, Augmentation of nucleate boiling heat transfer and critical heat flux using nanoparticle thin-film coatings, *International Journal of Heat and Mass Transfer*, 53 (2010) 58-67.

[13] A. Suriyawong and S. Wongwises, Nucleate pool boiling heat transfer characteristics of TiO_2-water nanofluids at very low concentrations, *Experimental Thermal and Fluid Science*, 34 (2010) 992-999.

[14] V. Trisaksri and S. Wongwises, Nucleate pool boiling heat transfer of TiO_2-R141b nanofluids, *International Journal of Heat and Mass Transfer*, 52 (2009) 1582-1588.

[15] S. M. You and J. H. Kim, Effect of nanoparticles on critical heat flux of water in pool boiling heat transfer, *Applied Physics Letters*, 83 (2003) 3374-3376.

[16] W. T. Wu, Y. M. Yang and J. R. Maa, Nucleate pool boiling enhancement by means of surfactant additives, *Experimental Thermal and Fluid Science*, 18 (1998) 195-209.

[17] J. M. Borsari and P. Friedman, Surfactant effects on critical and minimum heat flux, *Journal of Enhanced Heat Transfer*, 17 (2010) 293-300.

[18] Y. M. Yang and J. R. Maa, Pool boiling of dilute surfactant solutions, *Journal of Heat Transfer*, 105 (1983) 190-192.

[19] H. S. Lin, W. T. Wu, Y. M. Yang and J. R. Maa, Effect of surfactant additive on boiling in the case of quenching in subcooled water, *Proceedings of the Third International Symposium on Multiphase Flow and Heat Transfer*, Xi'an Jiaotong University Press (1994) 464-473.

[20] D. G. Kang, J. H. Kim and C. Y. Lee, Minimum film boiling temperature and minimum heat flux in pool boiling of high-temperature cylinder quenched by aqueous surfactant solution, *Journal of Mechanical Science and Technology*, 32 (2018) 5919-5926.

[21] C. Y. Lee and J. H. Kim, Investigation on minimum film boiling point of highly heated vertical metal rod in aqueous surfactant solution, *Transactions of the Korean Society of Mechanical Engineers B*, 41 (9) (2017) 597-603 (in Korean).

[22] J. V. Beck, B. Blackwell and C. R. St. Clair Jr., *Inverse Heat Conduction: Ill-Posed Problems*, John Wiley & Sons (1985).

[23] NIST Chemistry WebBook, SRD 69, *Thermophysical Properties of Fluid Systems*, U. S. Secretary of Commerce, USA (2018).

[24] V. M. Wasekar and R. M. Manglik, The influence of additive molecular weight and ionic nature on the pool boiling performance of aqueous surfactant solutions, *International Journal of Heat and Mass Transfer*, 45 (2002) 483-493.

[25] R. Freud, R. Harari and E. Sher, Collapsing criteria for vapor film around solid spheres as a fundamental stage leading to vapor explosion, *Nuclear Engineering and Design*, 239 (2009) 722-727.

[26] H. Jouhara and B. P. Axcell, Film boiling heat transfer and vapour film collapse on spheres, cylinders and plane surfaces, *Nuclear Engineering and Design*, 239 (2009) 1885-1900.

[27] I. Sher, R. Harari, R. Reshef and E. Sher, Film boiling collapse in solid spheres immersed in a sub-cooled liquid, *Applied Thermal Engineering*, 36 (2012) 219-226.

[28] S. J. Kline, The purpose of uncertainty analysis, *Journal of Fluids Engineering*, 107 (2) (1985) 153-160.

[29] Wikipedia, *Sodium Dodecyl Sulfate*, Wikimedia Foundation, Inc. (2020).

[30] S. M. Ghiaasiaan, *Two-Phase Flow, Boiling, and Condensation: In Conventional and Miniature System*, Cambridge University Press., Cambridge, United Kingdom (2007).

[31] Y. M. Qiao and S. Chandra, Experiments on adding a sur-

factant to water drops boiling on a hot surface, *Proceedings of the Royal Society of London, Series A: Mathematical, Physical and Engineering Sciences*, 453 (1997) 673-689.

Dong Gu Kang received a Ph.D. degree in the Department of Nuclear and Quantum Engineering from KAIST. Currently, he is a Principal Researcher of Korea Institute of Nuclear Safety.

Sunwoo Kim earned his Ph.D. degree in Mechanical Engineering and Materials Science from Duke University, USA in 2008. Currently, he works as an Associate Professor in the Mechanical Engineering Department at the University of Alaska, Fairbanks.

Chi Young Lee received a Ph.D. degree in the Department of Mechanical Engineering from KAIST. Currently, he is an Associate Professor in the Department of Fire Protection Engineering at Pukyong National University.